A Process-Aware Comparison of Mountain Precipitation Estimates in The East River Watershed

Presenter Name, William Rudisill*
Coauthors: Alejandro Flores*,
Affiliations: *Boise State University, Boise, ID, USA;
Email: williamrudisill@u.boisestate.edu

Introduction

- Precipitation is in general poorly quantified in areas of complex terrain This study examines differences in precipitation and temperature estimates across three commonly used datasets in addition to a *dynamically downscaled regional climate reconstruction* for water year 2017 (October 1-September 30).
- We compare Weather Research and Forecasting (WRF) model simulations with the Parameter Regression on Independent Slopes (PRISM), National Land Data Assimilation Version II (NLDASv2), and Daymet data products (See Table 1 for details).
- This study serves as a preliminary evaluation of an ongoing 20 year WRF simulation, while recognizing that the comparison datasets are themselves an estimate of truth.

Study Area: The East River Watershed, Colorado

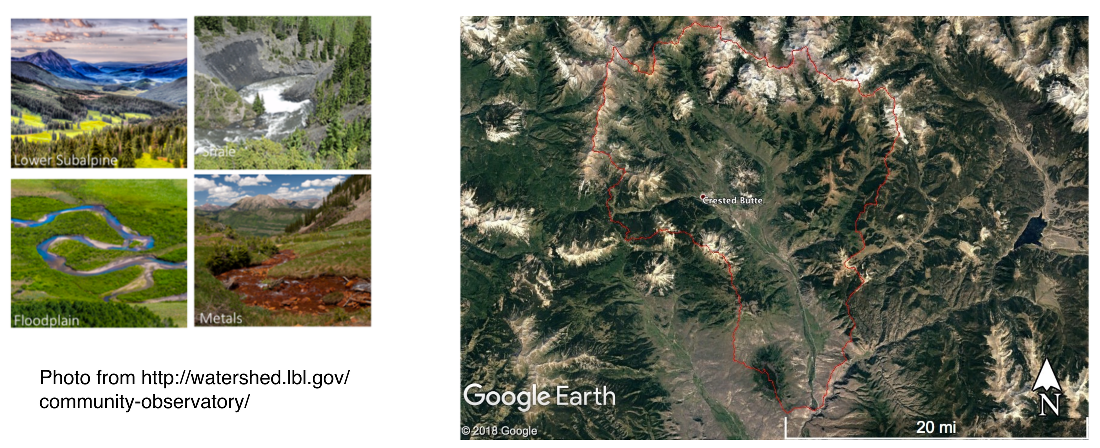

Photo from http://watershed.lbl.gov/community-observatory/

Figure 1: The many environments within the the East River Watershed. Steep topographic gradients and aspect variability cause large gradients in precipitation, temperature, soil structure, and ecosystem functional type.

The Weather Research and Forecasting Model

Figure 2: The WRF Model Domain topography (m) and the outline of the East River Watershed.

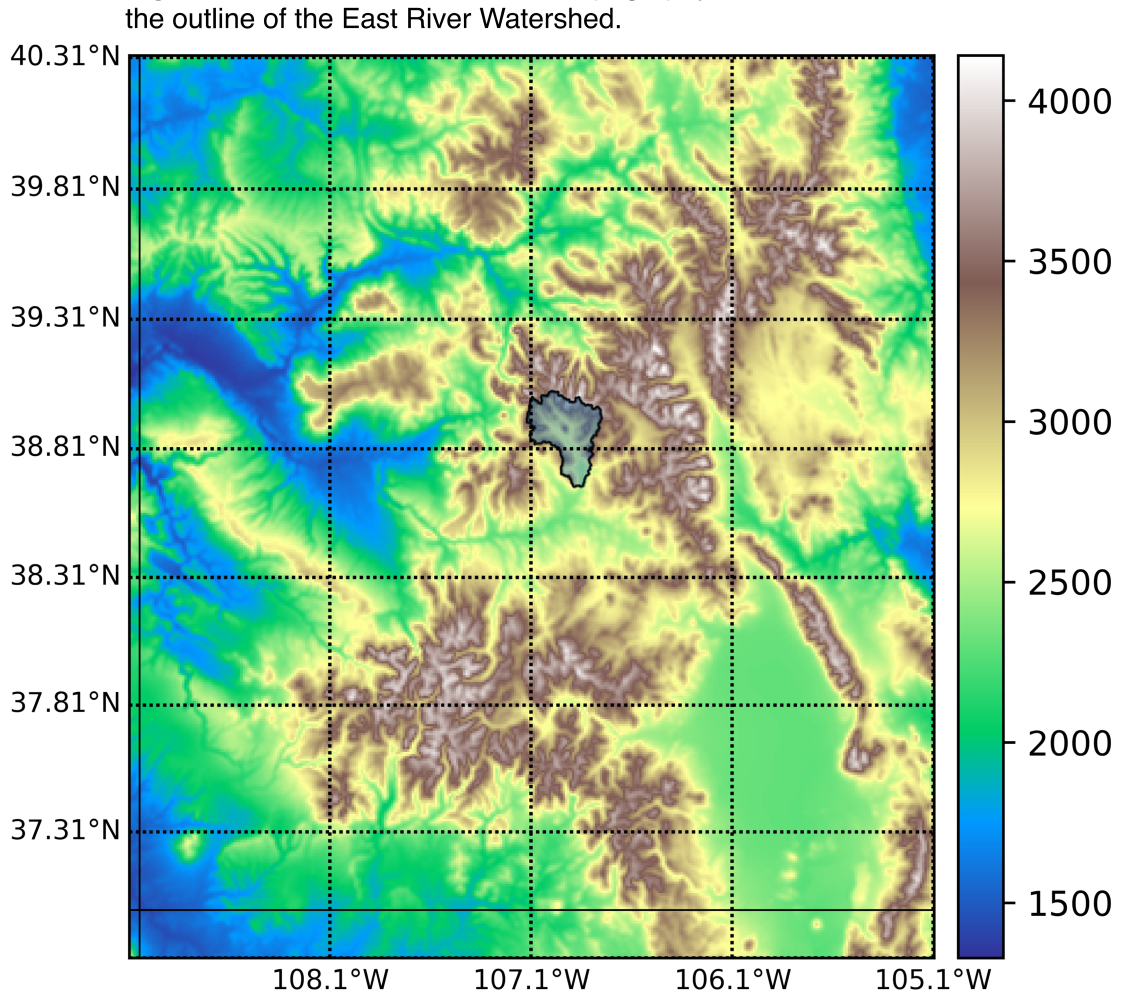

- The WRF (Weather Research and forecasting model) has demonstrated efficacy in simulating mountain precipitation (rain and snow) in a variety of locales (Ikeda, 2010)
- This WRF configuration uses a two-way nested 1km and 3km grids (the inner grid is show in Figure 2), 50 vertical levels, and Climate Forecast System Reanalysis (CFSR) boundary conditions.
- The convection parameterizations have been turned off, given that the grid resolution is below the 4km typically considered necessary to resolve convective storm events. (Prein et al. 2015)

Comparison Between WRF and Reference Datasets

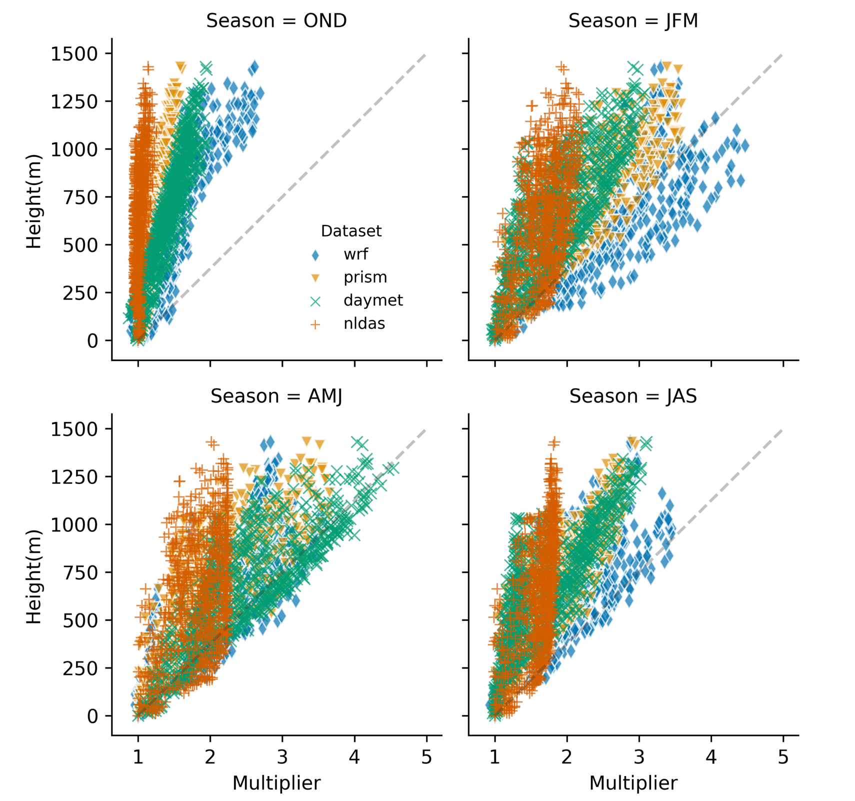

Figure 3.1: Average precipitation by season as a multiple of valley bottom precipitation, with respect to elevation. The dashed line is approximately 2x per 250 meters of elevation gain.

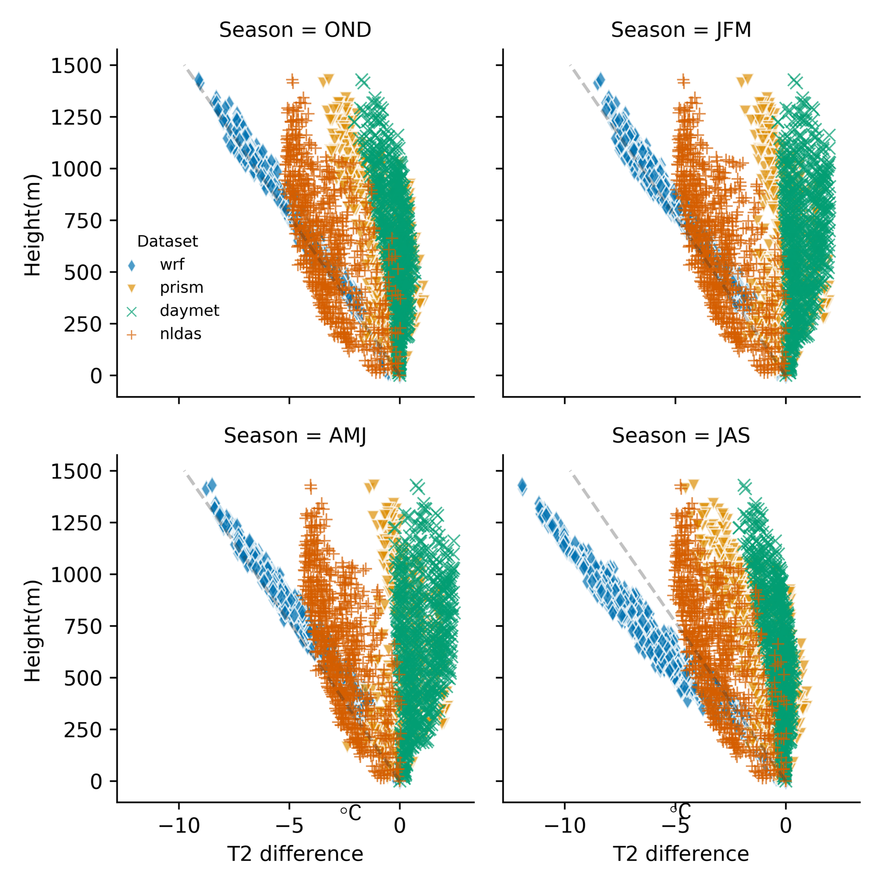

Figure 3.2: The seasonally averaged two meter daily minimum temperature with respect to vertical distance from the valley-bottom for each product. The dashed line is the -6.5*C/km adiabatic lapse rate.

Background

- Elevation gradients induce enhanced precipitation through a variety of mechanisms (See Houze (2012) for a review)
- Elevation likewise strongly impacts temperature, approximately proportional with change in pressure (-6.5*C/km for dry adiabatic conditions)
- Geostatisical meteorological products interpolate sparse station measurements using various weighting factors designed to account for orographic controls on precipitation and temperature.
- See **Table 1** for a description of the various products used in this study

Methods

- Data from DayMet, PRISM, NLDASV2 were acquired for water year 2017.
- All data are interpolated to the 1-km spatial resolution of the WRF modeling grid.
- WRF and NLDAS are aggregated to daily time steps, and we computed statistics on this basis.

Evaluation Metrics

- We evaluate the orographic precipitation gradient (OPG) between the various products by plotting mean seasonal precipitation for each grid cell as the multiple of the valley bottom precipitation, with respect to height above valley-bottom. (Figure 3.1, left)
- The same is done for seasonally averaged Tmin. The dry adiabatic lapse rate is shown as well (dashed line). Tmax has been computed, but is not shown. Daymet does not provide a Tmean product, which is why we currently only evaluate Tmin/max.
- The map-views display the mean water year bias between each pair of datasets, i.e, E([WRF-daymet, WRF-prism, WRF-nldas]).
- Total water year precipitation bias is computed in Figure 4, whereas the mean daily Tmin/Tmax bias is shown in Figure 5.

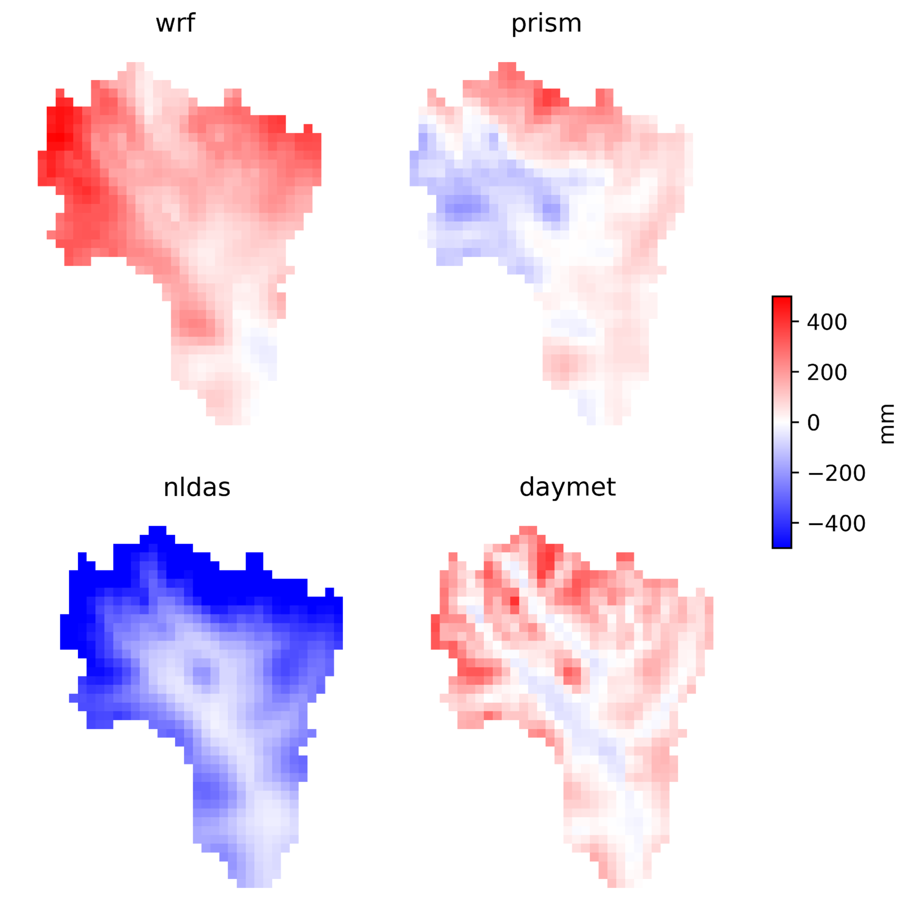

Figure 4: The average water year 2017 total precipitation bias for each dataset. The average bias is computed as the mean of the biases between each data product. Positive values (red) indicate that the dataset is warmer on average than the other datasets in for location, and negative values (blue) indicate the opposite.

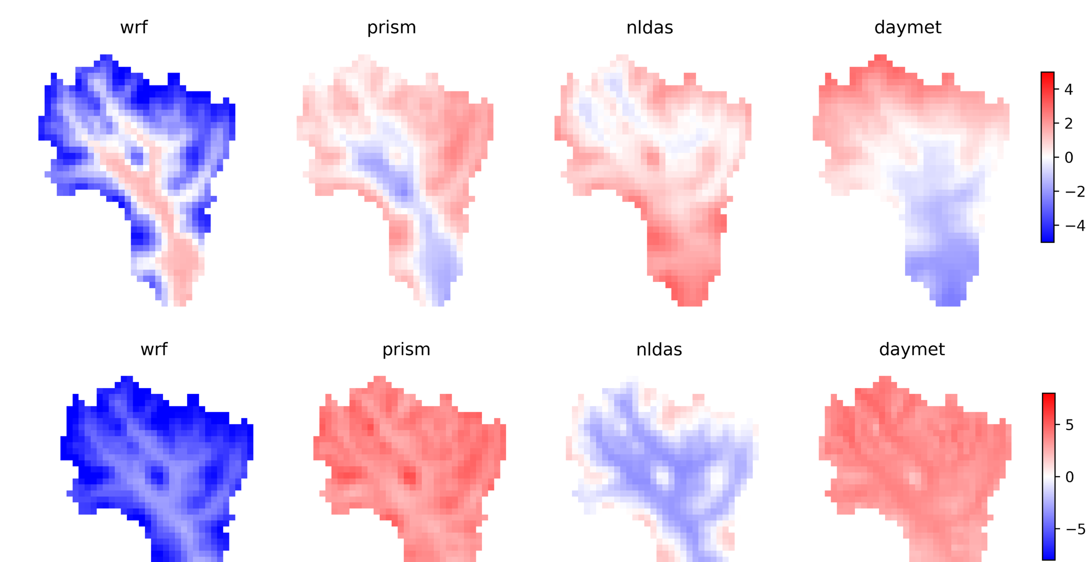

Figure 5. Same as figure 4, but for daily average Tmin (top) and Tmax (bottom). The average bias is computed as the mean of the biases between each data product. Positive values (red) indicate that the dataset is warmer on average than the other datasets in for location, and negative values (blue) indicate the opposite.

Results

- WRF Tmin closely follows the adiabatic lapse rate for each season (Figure 3.2)
- Orographic enhancement factors vary by season (Figure 3.1), and WRF consistently shows the highest rates of orographic enhancement and the highest variance within elevation ranges (not shown).
- NLDAS shows a clear "cut-off" value at a factor of ~2 times the valley bottom precipitation (Figure 3.1)

Future Work: Characterizing Orographic Precipitation Mechanisms In the East River

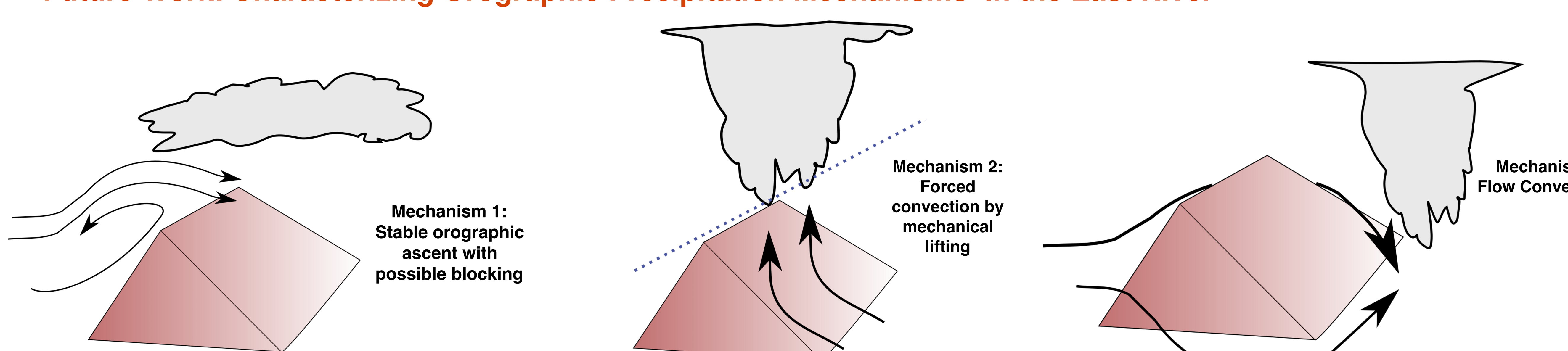

Figure 6. Select, idealized mechanisms of orographic precipitation. Figure adapted from Roe, 2005. Future work will quantify precipitation magnitude and frequency in light of these mechanisms.

Mechanism	Rationale	Diagnostic
Stable Orographic Ascent	What fraction of precipitation events are *blocked* (if any), and how does 'upstream' stability relate to observed precipitation? Blocking occurs during weak winds and strong static stability (Fr<1)	Compute Froude Number, where U is the normal-to -topography wind speed, N is the Brunt-Vaisala frequency, and H is the ridge height. $Fr = \frac{U}{Nh}$
Forced Convection	Potential instability in otherwise stable air can be released as released as the parcel is forced to ascent the mountain barrier, triggering convection.	Compute upstream regions of potential instability, defined by regions where equivalent potential temperature (theta) decreases with height (z). $\frac{d\theta_e}{dz} < 0$
Flow Convergence	Thermally driven, convergent flows and lee-side convergence may be important mechanisms triggering convection in mountain terrain.	Compute convergence of the 10m wind field for A particular region, A, around the East River. V Is the 10m wind field, and n is the unit normal vector directed Inwards toward the region A. $-\nabla \cdot \mathbf{v} = \frac{1}{A}\oint_A \mathbf{v} \cdot \hat{n} dA$

Station Observation Comparisons

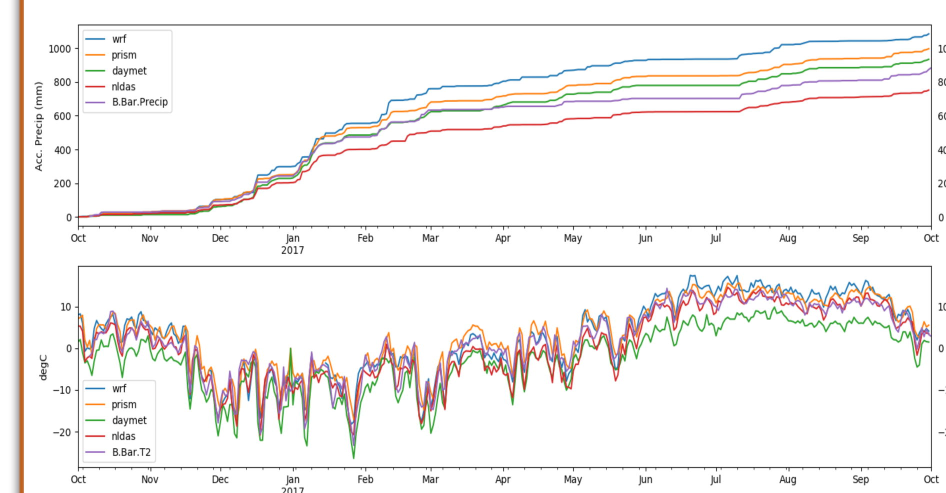

The Billy Bar meteorological station, looking north. Photo and data from the Western Regional Climate Center (https://wrcc.dri.edu/cgi-bin/rawMAIN.pl?corbil). The station is located at (38.963056, -106.993333), at ~9550 feet above sea level

Figure 8: Comparisons between the Billy Bar meteorological station and the corresponding grid cell for each data product. **Top:** Total Accumulated precipitation during water year 2017, and **Bottom:** Daily average two meter are temperature. Daymet does not provide two meter air temperature product, so the average of daily minimum and maximum temperature is used in its place.

Datasets Comparison

Dataset	Resolution	Data Sources	Notes	References
PRISM (AN81d, vD2)	Daily 4km	• Multiple gauge locations including NCRS Snotel. • Daily precipitation post 2002 uses NWS radar precipitation estimates	• PRISM precipitation interpolation methodology takes into account geographic position and rain shadows • Additionally, the daily PRISM data uses a 'climatologically-aided interpolation (CAI)' method based on long term estimates of climate normals • Temperature lapse rates are determined by regressions between stations • A new PRISM daily temperature dataset has been distributed as of October 2019 designed to mitigate biases in Snotel station temperature errors. • Data accessed from: http://www.prism.oregonstate.edu/recent/	Daly, Christopher, G. H. Taylor, and W. P. Gibson. "The PRISM approach to mapping precipitation and temperature." Proc., 10th AMS Conf. on Applied Climatology. 1997. Further documentation: http://www.prism.oregonstate.edu/documents/PRISM_datasets.pdf
NLDAS-2	Hourly 4km	• NWS Doppler radar • NOAA CMORPH (Satellite IR) • NOAA Climate Prediction Center (CPC) Daily Gauge Analysis • NWS NARR (weather model)	• NLDAS uses the PRISM interpolation methodology, but does *not* ingest Snotel data sources (the highest elevation stations in the Western US) • NLDAS uses a -6.5 C/km lapse rate to distribute temperature estimates across terrain.	Cosgrove, Brian A., et al. "Real-time and retrospective forcing in the North American Land Data Assimilation System (NLDAS) project." Journal of Geophysical Research: Atmospheres 108.D22 (2003). Technical note describing precipitation data methods: https://ldas.gsfc.nasa.gov/nldas/v2/forcing#AppendixC
Daymet	Daily 1km	• NOAA National Centers for Environmental Information's Global Historical Climatology Network (GHCN)-Daily dataset. (Gauge data)	• Uses a truncated Gaussian weighting filter to interpolate station precipitation observations across space. • Temperature lapse rates are determined by regressions between stations • Accessed from https://daymet.ornl.gov/	Thornton, P.E., M.M. Thornton, B.W. Mayer, Y. Wei, R. Devarakonda, R.S. Vose, and R.B. Cook. 2016. Daymet: Daily Surface Weather Data on a 1-km Grid for North America, Version 3. ORNL DAAC, Oak Ridge, Tennessee, USA. https://doi.org/10.3334/ORNLDAAC/1328
WRF v3.8.1 (used in this study)	Hourly 1km**	Climate Forecast System Reanalysis (CFSRv2)	**Model Configuration** - 50 vertical levels - ~300x300 inner grid dimensions at 1-km spatial resolution - CFSRv2 lateral boundary conditions - ~2 weeks spinup period prior to the start of WY2017	Skamarock, W. C., J. B. Klemp, J. Dudhia, D. O. Gill, D. M. Barker, M. G Duda, X.-Y. Huang, W. Wang, and J. G. Powers, 2008: A Description of the Advanced Research WRF Version 3. NCAR Tech. Note NCAR/TN-475+STR, 113 pp.

Table 1: Descriptions of the Datasets used in this paper. Lundquist et al (2015) provides a valuable literature review and these different precipitation datasets and their respective assumptions.

Conclusions

1. Other daily meteorological products exist, but have not been examined. A majority use PRISM climate normals in some capacity to aid in interpolation (Lundquist et al 2017).
2. There is substantial disagreement between geostatistical datasets, on the order of 200mm/year in the high elevation reaches of the East River watershed despite similar data sources (Table 1)
3. Some of the spatial error patterns are likely associated with the different product resolutions (see Table 1).
4. NLDAS artificially 'saturates' at an orographic precipitation enhancement factor of two. Unlike PRISM, NLDAS does not assimilate the high elevation Snotel station observations.
5. None of the gridded datasets represent 'Truth'. However, these results suggest that this configuration of WRF is reasonably capturing meteorological conditions in this region, especially in terms of precipitation.
6. More observations should be directed to the mountain ranges in the northwest corner of the watershed to better precipitation magnitudes, orographic precipitation enhancement factors, and surface temperature lapse rates.
7. While the results shown are relevant to the East River, the methods are extensible to other mountainous regions.

References

1. Prein, Andreas F., et al. "A review on regional convection-permitting climate modeling: Demonstrations, prospects, and challenges." Reviews of Geophysics 53.2 (2015): 323-361.
2. Ikeda, Kyoko, et al. "Simulation of seasonal snowfall over Colorado." Atmospheric Research 97.4 (2010): 462-477.
3. Daly, Christopher, G. H. Taylor, and W. P. Gibson. "The PRISM approach to mapping precipitation and temperature." Proc., 10th AMS Conf. on Applied Climatology. 1997.
4. Lundquist, Jessica D., et al. "Relationships between barrier jet heights, orographic precipitation gradients, and streamflow in the northern Sierra Nevada." Journal of Hydrometeorology 11.5 (2010): 1141-1156.
5. Lundquist, Jessica D., et al. "High-elevation precipitation patterns: Using snow measurements to assess daily gridded datasets across the Sierra Nevada, California." Journal of Hydrometeorology 16.4 (2015): 1773-1792.
6. Houze Jr, Robert A. "Orographic effects on precipitating clouds." Reviews of Geophysics 50.1 (2012).

Acknowledgements:

- The authors acknowledge support for this research from the Department of Energy Subsurface Biogeochemical Research Program award DE-SC0019222
- This research made use of the resources of the High Performance Computing Center at Idaho National Laboratory, which is supported by the Office of Nuclear Energy of the U.S. Department of Energy and the Nuclear Science User Facilities under Contract No. DE-AC07-05ID14517.

Lab for Ecohydrological Applications and Forecasting

BOISE STATE UNIVERSITY